

## *Supplementary Material*

# Genome-wide analysis of transcriptome and histone modifications in *Brassica napus* hybrid

Meng Ma<sup>†</sup>, Wenying Zhong<sup>†</sup>, Qing Zhang, Li Deng, Jing Wen, Bin Yi, Jinxing Tu, Tingdong Fu, Lun Zhao and Jinxiong Shen<sup>\*</sup>

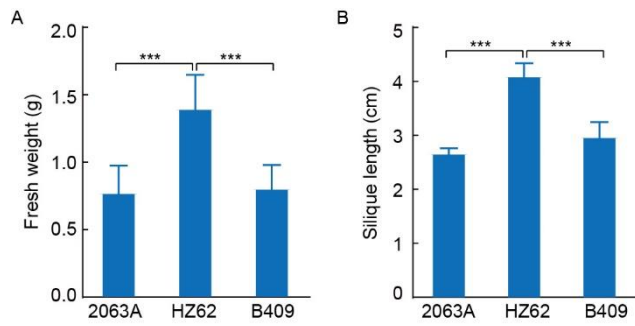
**\*Correspondence:**

Jinxiong Shen  
jxshen@mail.hzau.edu.cn

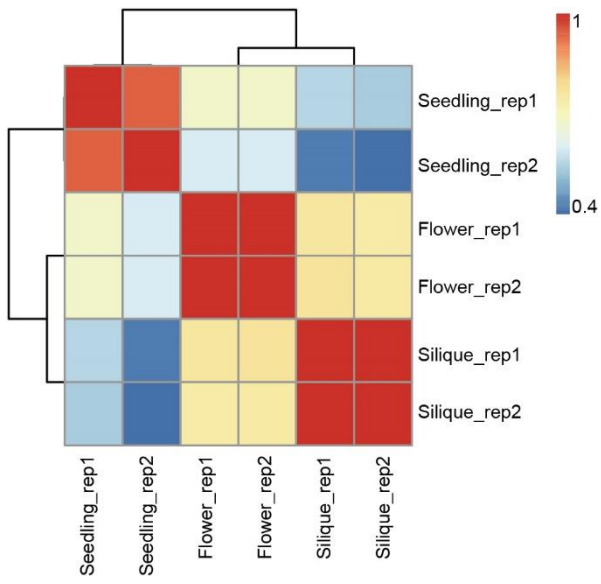
### Supplementary Figures



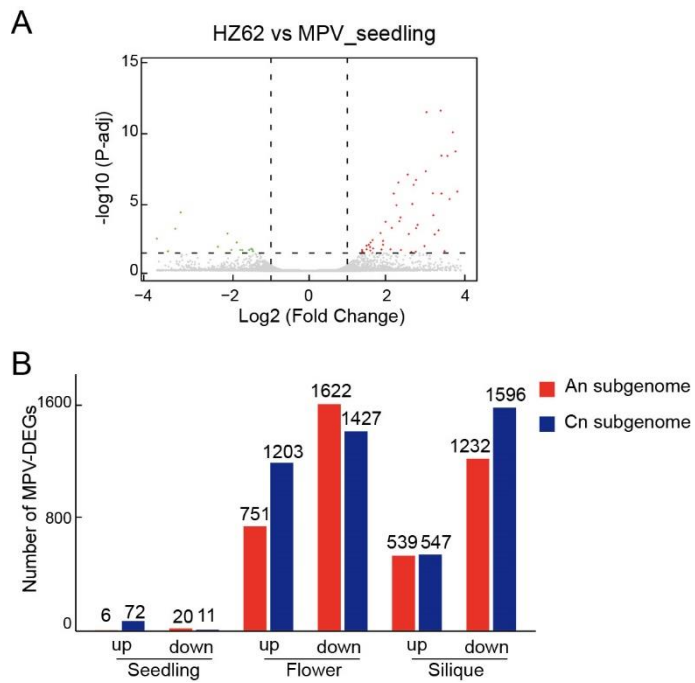
**Supplementary Figure 1.** Flower bud morphology in parents and their hybrid.



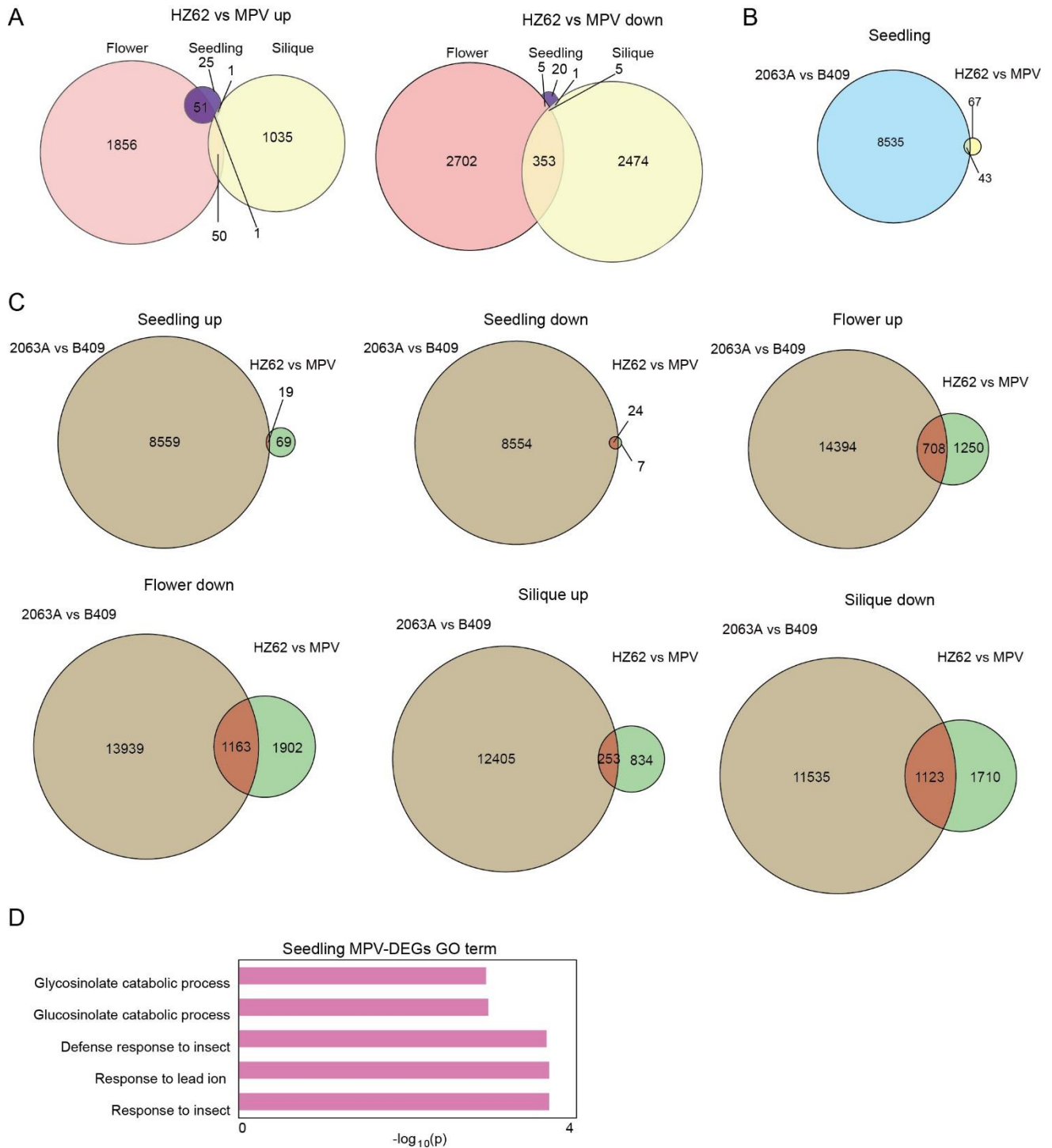
**Supplementary Figure 2.** Heterosis of hybrid in seedling and silique. **(A)** Comparison of fresh weight among parents and their hybrid. **(B)** Comparison of silique length among parents and their hybrid. The statistical analysis was performed using the t-test. \*\*\* $p < 0.001$ .



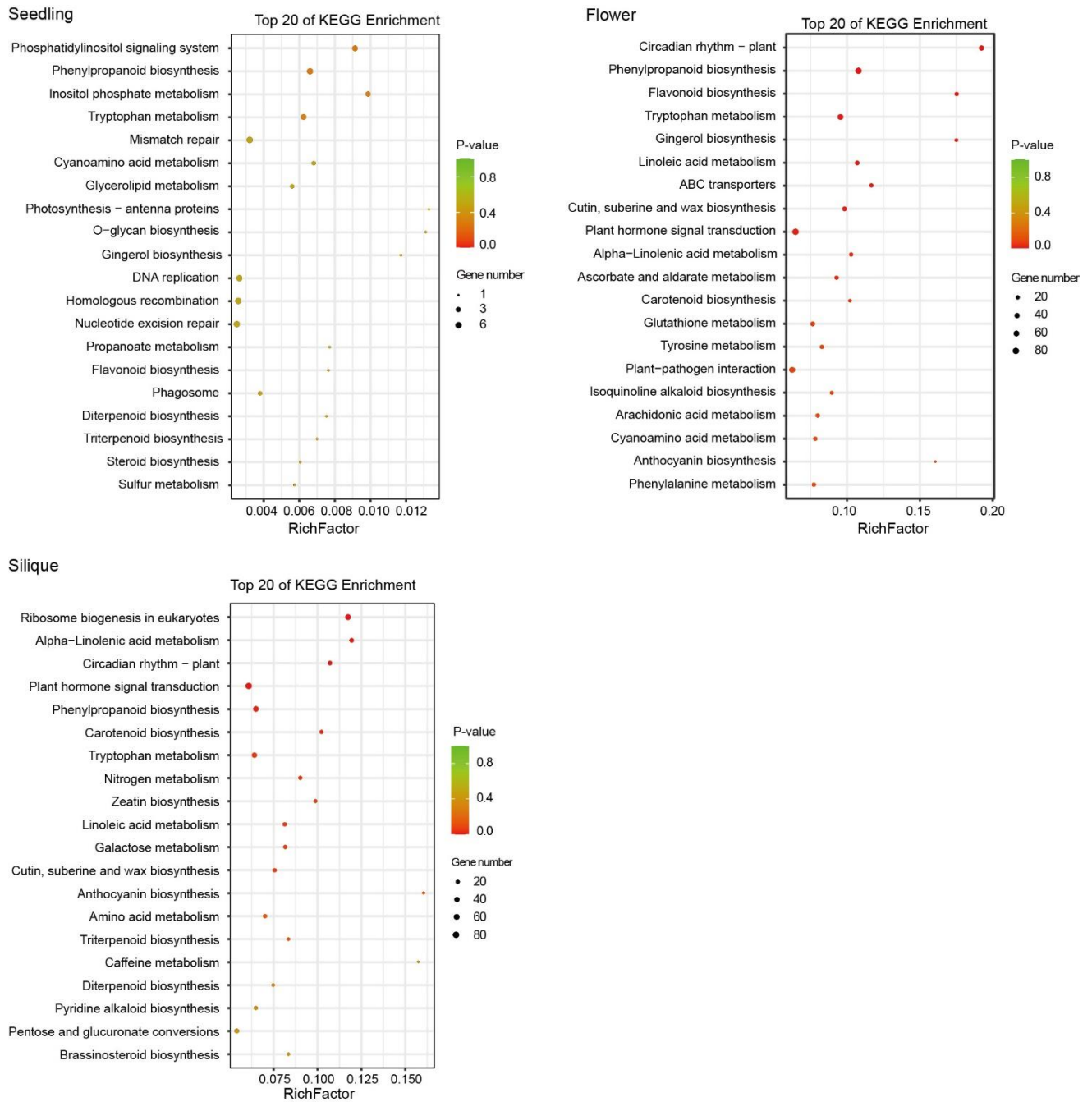
**Supplementary Figure 3.** Pearson correlation coefficient of RNA-seq.



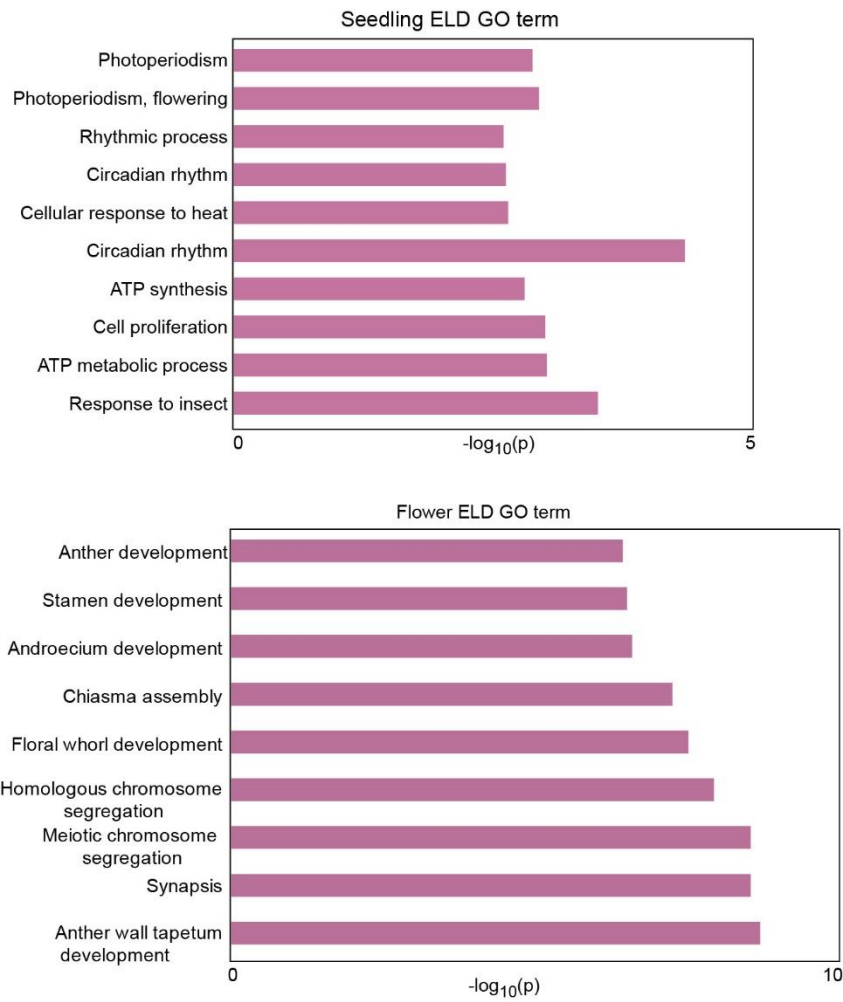
**Supplementary Figure 4.** MPV-DEGs in hybrid compared with parents. **(A)** Volcano plot of MPV-DEGs in hybrid seedling tissue. **(B)** Distribution of MPV-DEGs across the An and Cn subgenomes for all three tissues types.



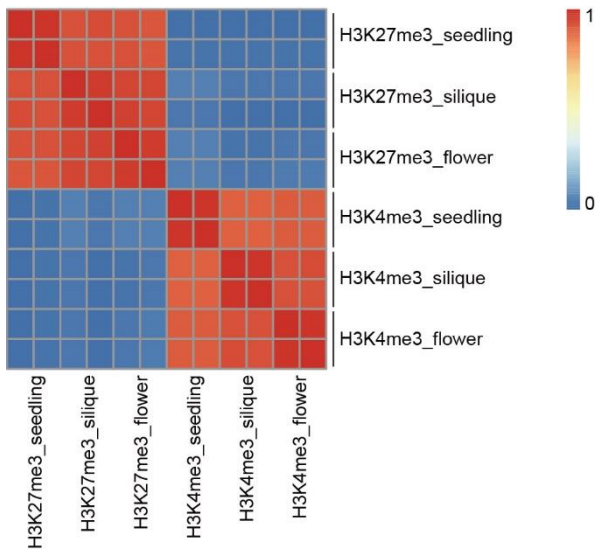
**Supplementary Figure 5.** MPV-DEGs in the hybrid. **(A)** Overlap of MPV-DEGs among three tissues. **(B)** Overlap of MPV-DEGs with parental DEGs in the indicated tissues. **(C)** Overlap of up-regulated and down-regulated MPV-DEGs with parental DEGs in seedling, flower bud, and silique tissues. **(D)** GO terms of MPV-DEGs in the silique.



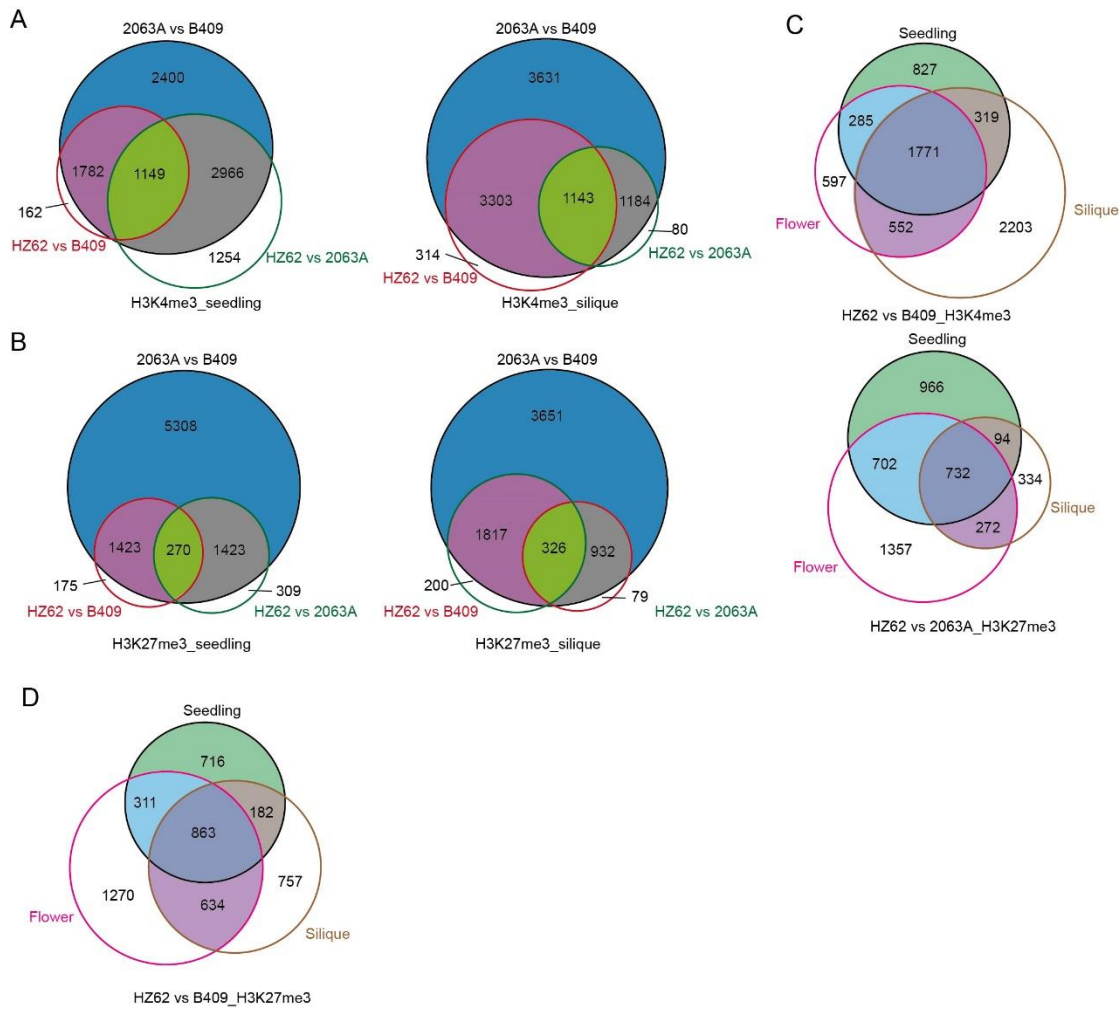
Supplementary Figure 6. KEGG analysis of MPV-DEGs in the indicated tissues.



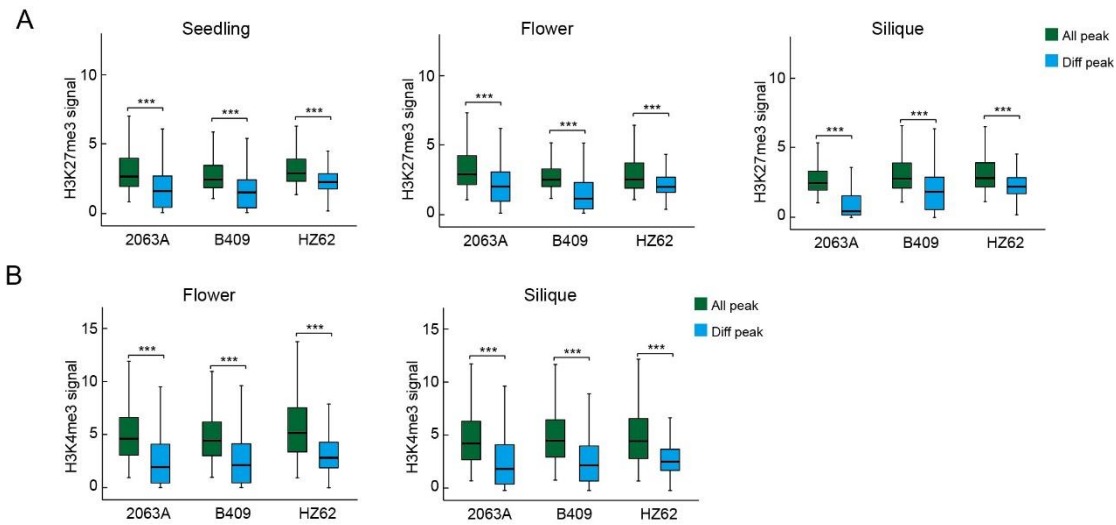
**Supplementary Figure 7.** GO analysis of ELD genes in seedling and flower bud.



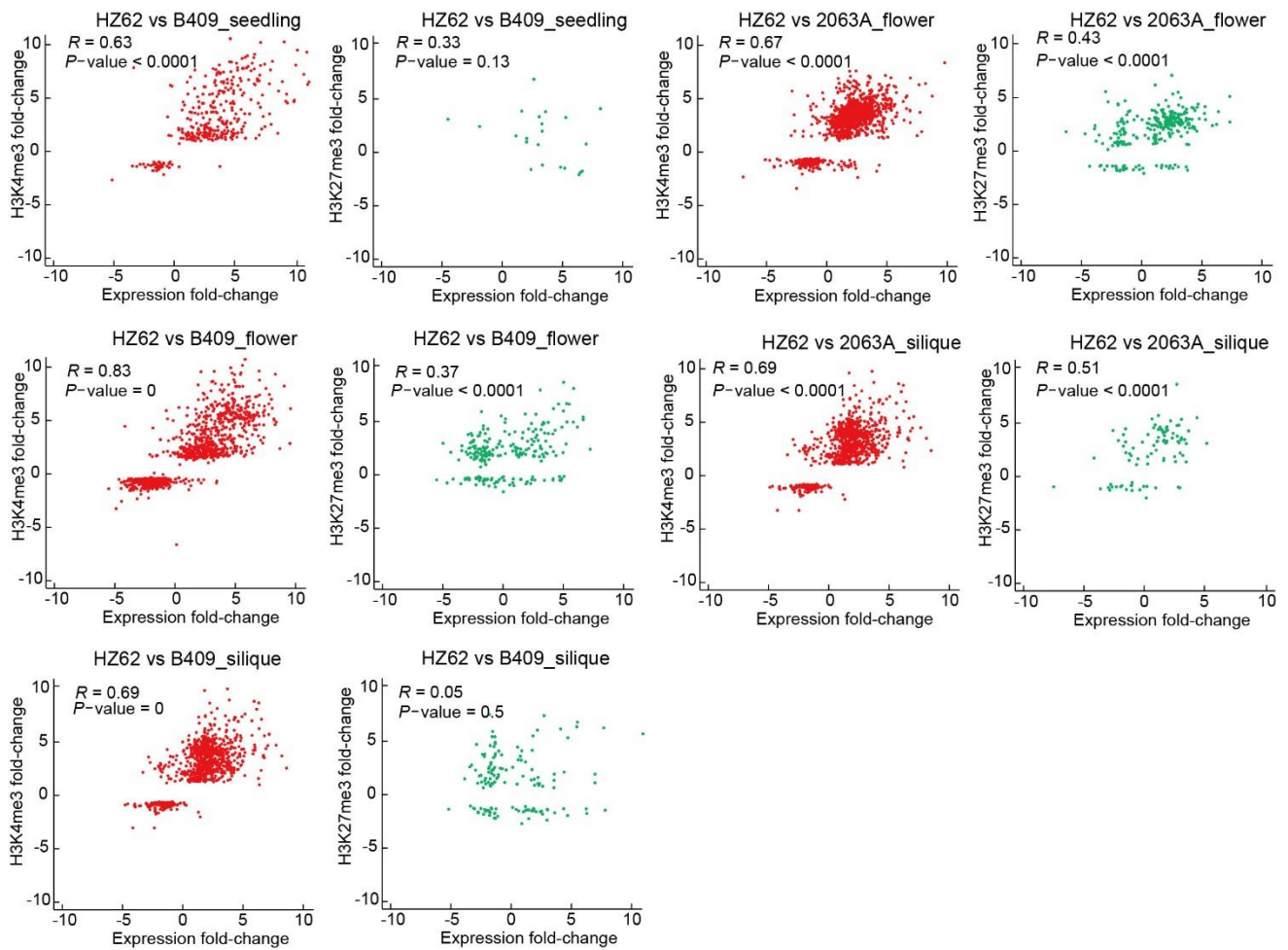
**Supplementary Figure 8.** Pearson correlation coefficient of ChIP-seq data.



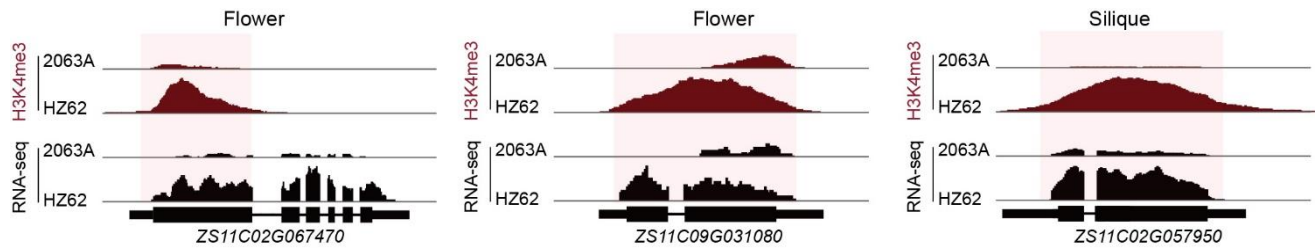
**Supplementary Figure 9.** Epigenetic variations in hybrid. **(A)** Venn diagram displaying the overlap of variation of H3K4me3 among parents and hybrid in the indicated tissues. **(B)** Overlap of variation of H3K27me3 among parents and hybrid in the indicated tissues. **(C)** Venn diagram displaying the overlap of variation of histone modifications between parents and hybrid for three tissue types.



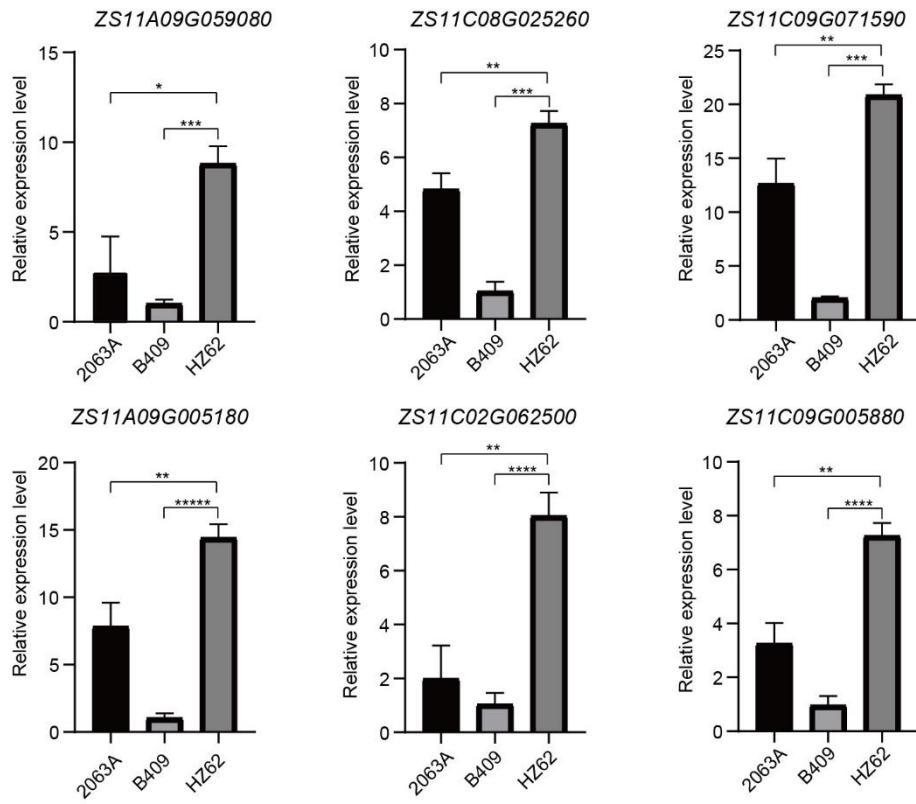
**Supplementary Figure 10.** The intensities of histone modifications in stable and variable regions. **(A)** Intensities of all and differential H3K4me3 peaks in the indicated varieties. **(B)** Intensities of all and differential H3K4me3 peaks in the indicated varieties. The statistical analysis was performed using the Wilcoxon test. \*\*\* $p < 0.001$ .



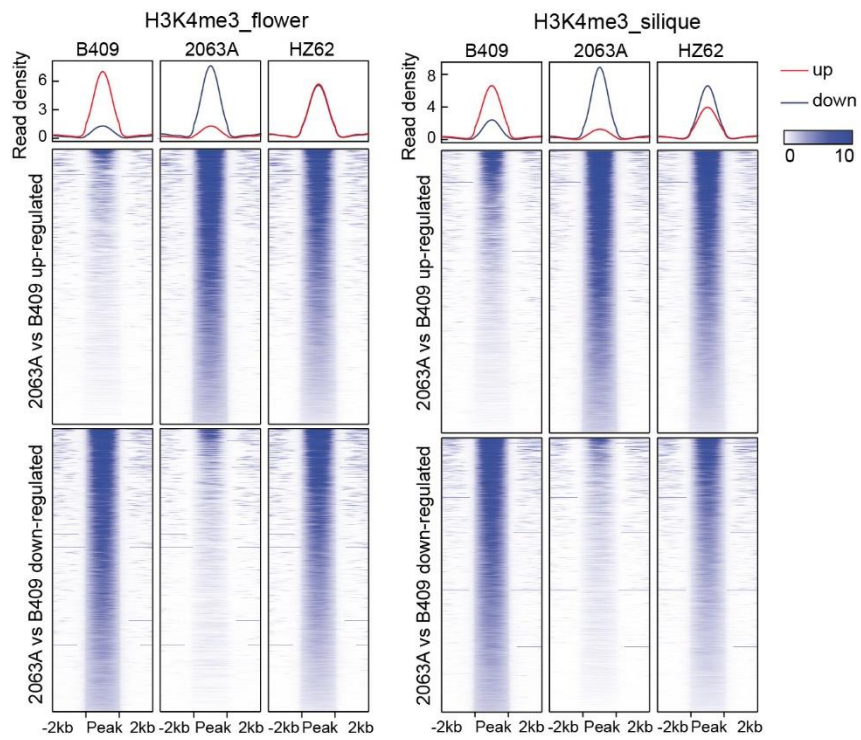
**Supplementary Figure 11.** Correlations between differential histone modification and gene expression. The statistical analysis was performed using the t-test.



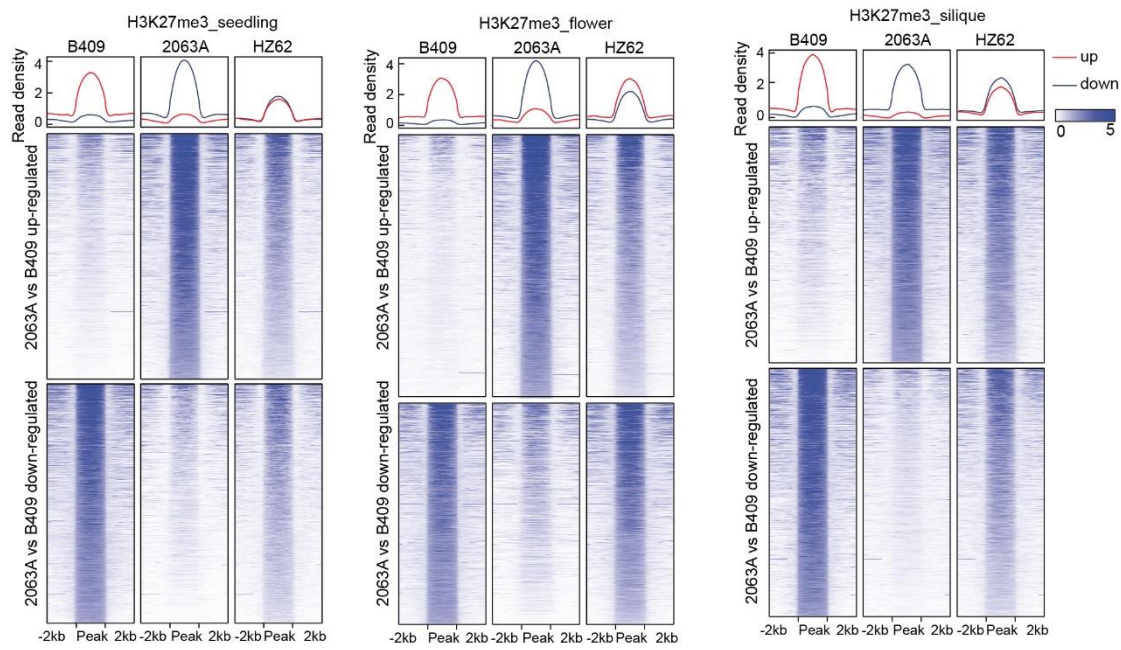
**Supplementary Figure 12.** Genome browsers of differentially H3K4me3-modified regions and expressed genes in HZ62 and 2063A.



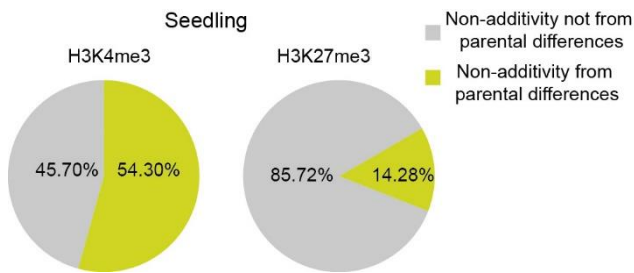
**Supplementary Figure 13.** Relative expression of starch metabolism related genes in parents and hybrid (\* $p < 0.05$ , \*\*\*\* $p < 0.0001$ ; t-test).



**Supplementary Figure 14.** Comparison of intensities of H3K4me3 in differentially histone-modified regions among parents and hybrid.



**Supplementary Figure 15.** Comparison of intensities of H3K27me3 in differentially histone-modified regions among parents and hybrid.



**Supplementary Figure 16.** The percentage of non-additively modified regions in hybrid originating from parental differentially histone-modified regions in the seedling.